Atomic Structure and Dynamics of Defects in 2D MoS_2 Bilayers

Si Zhou[1], Shanshan Wang[1], Huashan Li[2], Wenshuo Xu[1], Chuncheng Gong[1], Jeffrey C. Grossman[2], Jamie H. Warner[1]*

[1]Department of Materials, University of Oxford, 16 Parks Road, Oxford, OX1 3PH, United Kingdom

[2]Department of Materials Science and Engineering, Massachusetts Institute of Technology, 77 Massachusetts Avenue, Cambridge, Massachusetts 02139, United States

Email: *Jamie.warner@materials.ox.ac.uk

S1. Optical and SEM images of monolayer and bilayer regions in MoS_2

From the as-grown sample shown in Figure S1a, monolayer and few-layer MoS_2 coexist and are distinguished by optical contrast. Photoluminescence (PL) spectra in Figure S1b are obtained from monolayer and bilayer regions marked by red and black in the inset, respectively, further indicating the coexistence of monolayers and multilayers in our MoS_2 sample. The SEM image in Figure S1c demonstrates nucleation of another MoS_2 layer on top of the monolayer triangles. Low magnification TEM image indicates clear boundaries between monolayer and bilayer regions which matches the optical microscope result (Figure S1d).

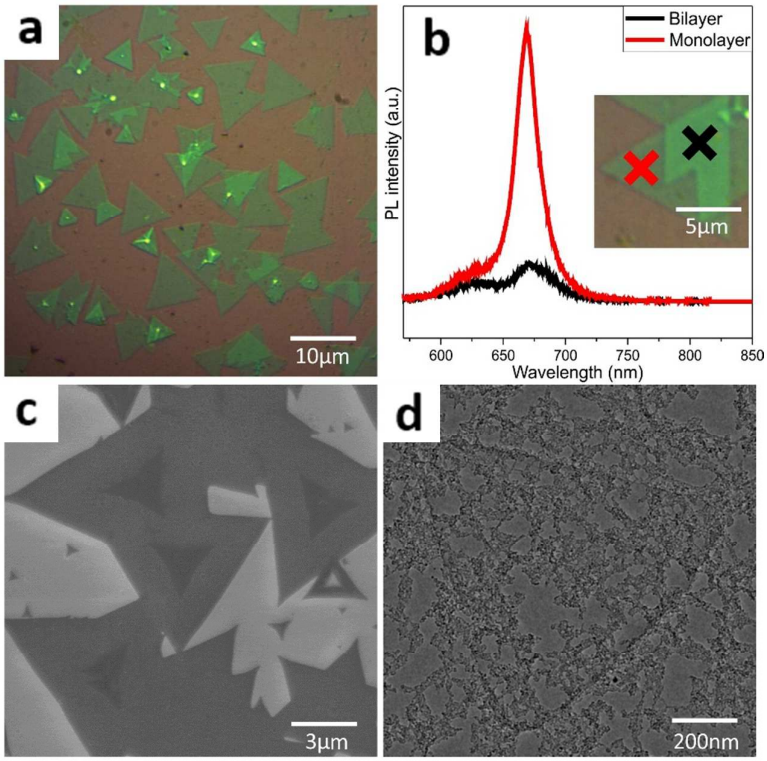

Figure S1. (a) Optical image of a CVD growth of typical MoS_2 triangles (a) SiO_2/Si (300 nm) substrate. (b)Photoluminescence spectra from monolayer and bilayer regions. (c) SEM image of triangular multilayers nucleated on top of monolayer MoS_2. (d) Low magnification TEM image showing an isolated triangular crystal on top of monolayer MoS_2.

S2. AC-TEM images of mono-bilayer interfaces in 2H and 3R MoS_2 bilayers

Two types of mono-bilayer step-edges were found in the AC-TEM images, Figure S2a and S2c, corresponding to 2H and 3R stacking respectively. The 2H stacked bilayer region shows the expected AA' ordering, while the 3R bilayer shows the AB stacking leading to a more complex contrast pattern than the AA'. Multislice image simulations based on the atomic models (Figures S2e-h) match the experimental ones, confirming the two stacking structures, with the line profiles of the experimental and simulated images compared in Figures S2i and j.

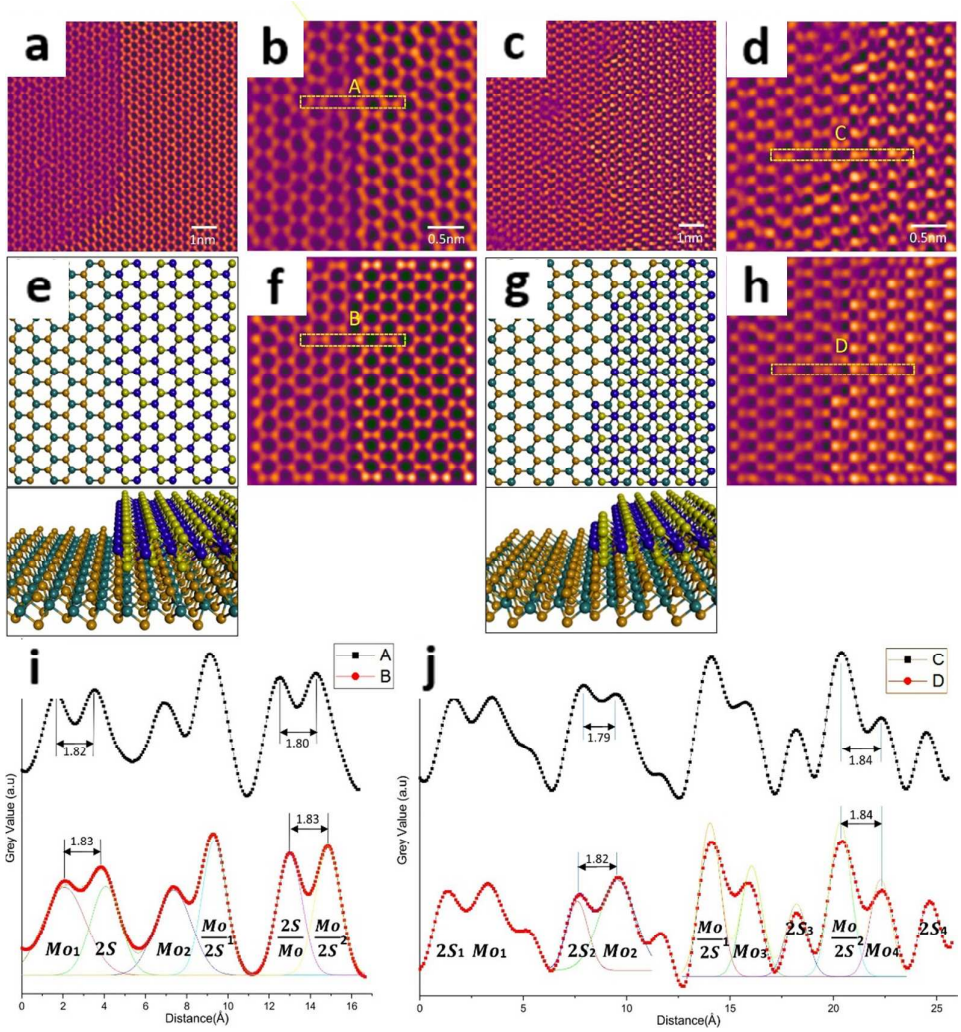

Figure S2. AC-TEM images of the MoS_2 monolayer-bilayer step edge for (a, b) 2H stacking and (c, d) 3R stacking. Atomic models from top and 3D view and corresponding multislice image simulations for (e, f) 2H stacking and (g, h) 3R stacking. (i) Boxed line profiles of the step edge in (b) and (f). (j) Boxed line profiles of the step edge in (d) and (h).

S3. Additional images of Sulphur vacancies in 2H and 3R bilayer MoS_2

In Figure S3, Line intensity profiles are taken from at least three sites of each type of Sulphur vacancies (SV/DV in 2H bilayer as well as SV_1/DV_1 and SV_2/DV_2 in 3R bilayer) in HRTEM images to get average peak intensity ratio. For SV and DV in 2H bilayer, the $(2S/Mo)_2/(Mo/S)$ and $(2S/Mo)_2/(Mo)$ ratio falls into 1.16-1.28 and 1.47-1.70. For SV_1, DV_1, SV_2 and DV_2 in 3R bilayer, the peak intensity ratio $(Mo)_1/(Mo/S)$, $(Mo)_1/(Mo)_2$, $(S)/(Mo)_2$ and $(V)/(Mo)_2$ (V

stands for vacuum) is in the range of 2.82-3.01, 1.80-2.11, 1.33-1.48 and 1.72-1.82, respectively. The intensity ratio matches that obtained in simulated images in figure 1f and g and figure 5j to m.

S4. AC-TEM images of 3R stacked MoS_2 under different focusing conditions

The image frames shown from figure S4a to S4e display the AC-TEM image frames of 3R stacking bilayer MoS_2 under different focusing conditions, with three columns (2S/Mo), (Mo) and (2S) showing varying contrast. Multislice image simulations of 3R bilayer MoS_2 ranging from figure S4f to S4j are conducted using defocus spread of 5nm and various defocus values to match the experimental results. For comparison, the simulated images of 2H bilayer MoS_2 (figure S4k-S4o) are conducted using the same defocus values. This provides additional evidence of the 3R stacking sequence existing in our sample.

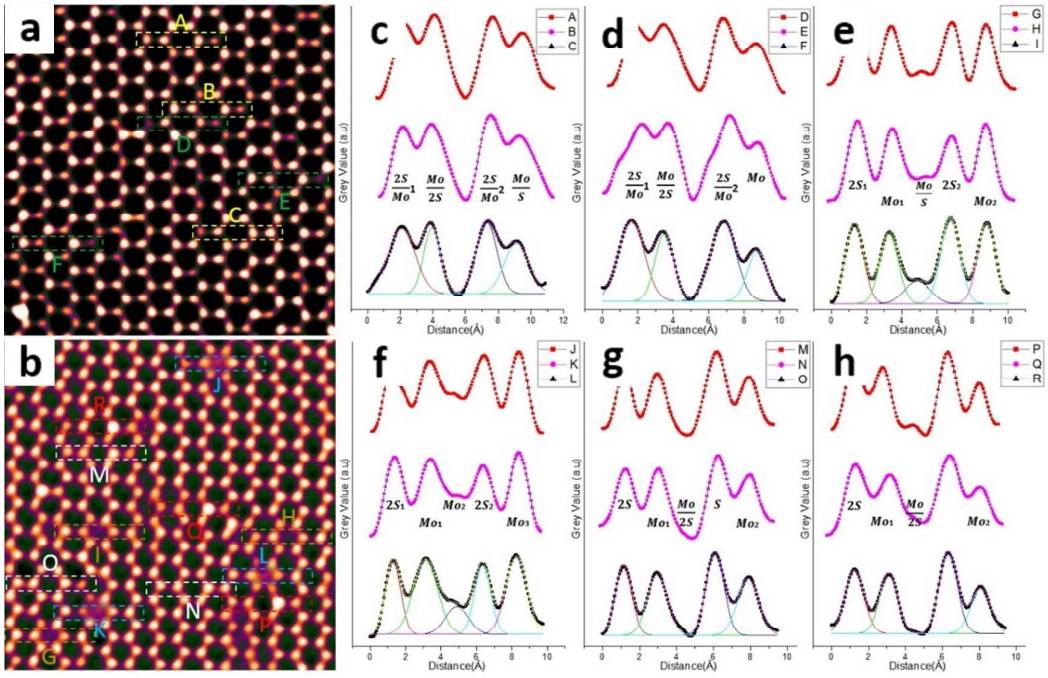

Figure S3. AC-TEM image showing SV/DVs in (a) 2H stacked bilayer MoS_2 as dim spot and (b) 3R stacked bilayer MoS_2 as blurry regions and bright spots. Line intensity profile taken along (c) yellow arrows and (d) green arrows in (a). Line intensity profiles taken along (e) brown arrows, (f) blue

arrows, (g) white arrows and (h) red arrows as marked in (b). Gauss fitting is applied for the peak intensity ratio measurement.

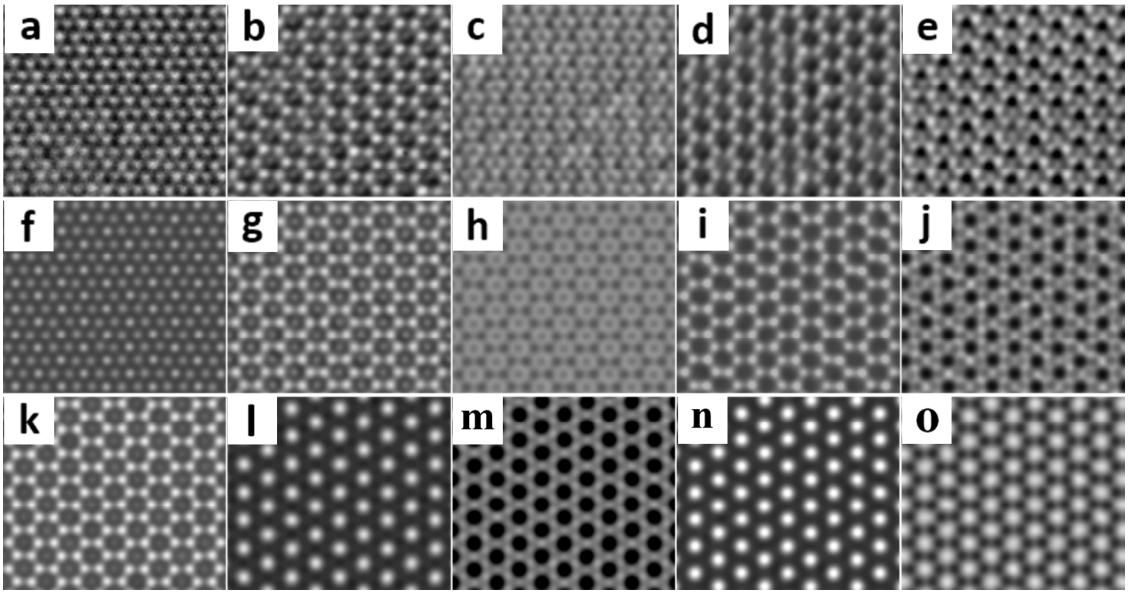

Figure S4. (a-e) TEM image showing unique contrast changes of 3R stacked bilayer MoS_2 under various focusing circumstances. Multislice image simulations under defocus value of -2, 7, -9, 10 and 4nm, respectively, for (f-j) 3R and (k-o) 2H stacked bilayer MoS_2. The defocus spread used is 5nm.

S5. Bond length measurement for defective monolayer and defective layer from bilayer

For monolayer with 1SVL (Figure S5a), the Mo-S bond length along the defective site ranges from 2.333 to 2.579 Å, implying that the maximum increase or shrinkage of bond length compared to pristine crystal (2.420 Å) is 6.6%, which is 3.7% for the defective layer from bilayer as shown in Figure S5b. This proves less in-plane compression introduced by 1SVL in bilayer system. Furthermore, the significant mismatch depicted in Figure 3e mainly derives from the out-out-plane lattice distortion.

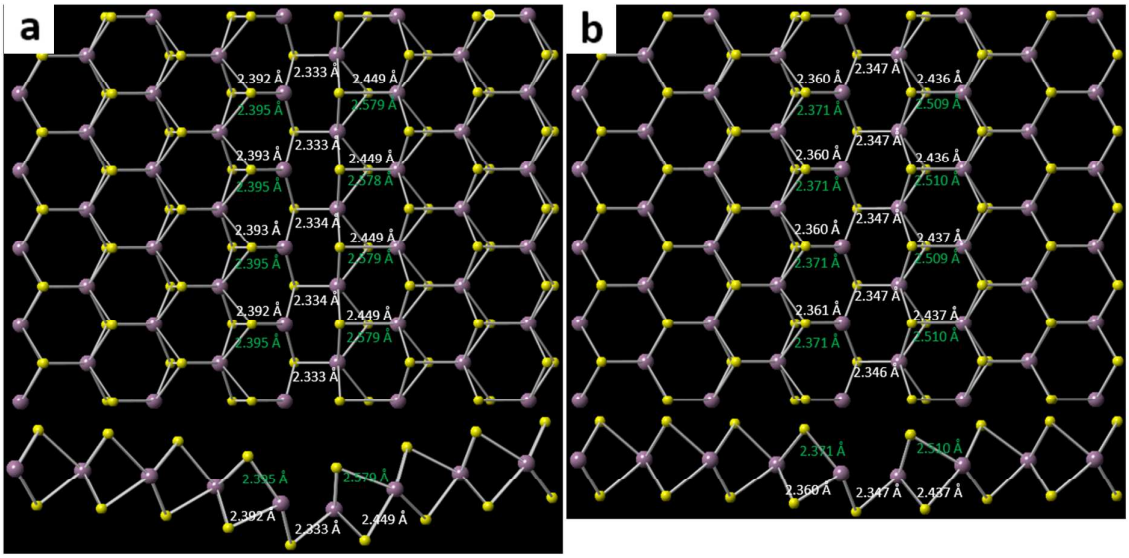

Figure S5. DFT-calculated models with 1SVL from both top and side view of (a) monolayer and (b) defective layer from 2H stacked bilayer MoS_2. Bond length is marked as white and green for Mo-S (bottom plane) and Mo-S (top plane), respectively. Standard Mo-S distance bond length is 2.420Å.